Journal of Magnetic Resonance 195 (2008) 1–8

Contents lists available at ScienceDirect

Journal of Magnetic Resonance

journal homepage: www.elsevier.com/locate/jmr

NMR relaxation interference effects and internal dynamics in γ-cyclodextrin

Leila Ghalebani, Dmytro Kotsyubynskyy, Jozef Kowalewski *

Department of Physical, Inorganic and Structural Chemistry, Arrhenius Laboratory, Stockholm University, S-10691 Stockholm, Sweden

ARTICLE INFO

Article history:
Received 13 June 2008
Revised 29 July 2008
Available online 12 August 2008

Keywords:
Carbon-13 relaxation
Cross-correlated relaxation
Molecular dynamics
Internal motion
Random jumps

ABSTRACT

Multiple-magnetic field (9.4, 14.1 and 21.1 T) measurements of ^{13}C spin–lattice and spin–spin relaxation rates, the heteronuclear Overhauser enhancement and cross-correlated relaxation rates (CCRRs) in the methylene groups are reported for γ-cyclodextrin in water/dimethylsulfoxide solution at 323 and 343 K. The CCRRs are obtained from differences in the initial relaxation rates of the components of the CH_2 triplet in the ^{13}C spectra. The relaxation data are analyzed using the Lipari–Szabo approach and a novel modification of the two-site jump model. According to the latter model, inclusion of the dipolar (CH,CH′) cross-correlated longitudinal and transverse relaxation is important for estimating the rate of the conformational jumps in the hydroxymethyl group. Using the dynamic information from the jump model, we have also used the differences in the initial relaxation rates for the triplet components to estimate the anisotropy of the chemical shielding tensor.

1. Introduction

In liquid state NMR, cross-correlated spin relaxation or relaxation interference phenomena can provide valuable information about molecular structure and dynamics. These effects have been known for long time [1–4] and are experimentally often observed as differential line widths or line intensities in *J*-coupled multiplets in NMR spectra. The cross-correlated relaxation phenomena arise through correlated fluctuations of different interactions and can be described in terms of polarization or coherence transfers [5–9]. Not least, these phenomena have during recent decades found important applications in NMR studies of the dynamics and structure of proteins and other biological molecules [10–12]. One of the groupings of interest are methylene groups, $^{13}CH_2$, commonly studied in uniformly ^{13}C-labeled proteins [6,13–20].

In a recent communication, we described a simple experimental methodology for studies of cross-correlated relaxation, suitable for methylene groups in smaller molecules and possible to use at natural abundance [21]. We have also applied these methods on some reasonably rigid molecules and investigated the consistency of the cross-correlated relaxation data with conventional heteronuclear relaxation properties (spin–lattice and spin–spin relaxation rates, nuclear Overhauser enhancement) for different molecules. The conventional relaxation data can also be referred to as auto-correlated relaxation parameters. Here, we turn our interest towards carbohydrates and their internal dynamics. Application of cross-correlated relaxation rates brings an additional tool for the structure determination and dynamical studies of carbohydrates. It appears especially suitable for studies of local conformational dynamics in oligosaccharides. We use here γ-cyclodextrin (γ-CD) as a model system (Scheme 1). γ-CD is a cyclic oligomer consisting of eight glucose residues which form a shallow truncated molecular cone of almost perfectly symmetrical structure [22].

The dynamics of cyclodextrins has earlier been studied by Kowalewski and Widmalm [23], using conventional ^{13}C relaxation parameters at several magnetic fields. In this study, we combine the conventional ^{13}C relaxation data with the longitudinal and transverse cross-correlated relaxation rates (CCRRs) and explore the possibilities that these extended experimental data sets offer in order to obtain a better understanding of important local conformational dynamics. This additional dynamics of exocyclic methylene group has been mentioned by McCain and Markley [24]. We studied previously the conformational dynamics of hydroxymethyl group, using cross-correlated relaxation rates, in a monosaccharide methyl-β-D-glucopyranoside [25] using a somewhat different experimental approach.

Interpretation of relaxation data, both conventional and CCRRs, requires appropriate dynamic models [26–29]. The task of interpreting relaxation data is reasonably simple for molecules which can be considered as rigid bodies undergoing rotational diffusion in small steps [21]. The presence of large-amplitude internal motions complicates the situation very significantly. In many cases, one chooses to use a simple model combining isotropic global reorientation by rotational diffusion with rapid and anisotropic local motions, developed independently by several groups [30–33] and widely known as the Lipari–Szabo model-free approach. In the investigation of methyl-β-D-glucopyranoside [25], we have used a "hybrid" model, where the Lipari–Szabo model was used for auto-correlated relaxation processes, while the cross-correlated

* Corresponding author. Fax: +46 8 163118.
E-mail address: jk@physc.su.se (J. Kowalewski).

1090-7807/$ - see front matter © 2008 Elsevier Inc. All rights reserved.
doi:10.1016/j.jmr.2008.07.025

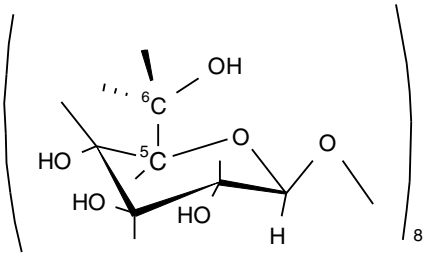

Scheme 1.

relaxation data were described by a jump model. In this study, we present a modified dynamic model which seems to function in a more consistent way.

The present article is organized in the following manner. Section 2 covers a brief theory. Section 3 deals with the experiments and explains how various relaxation parameters are obtained. In section 4, the experimental auto- and cross-correlated relaxation parameters are interpreted according to different motional models and the results are discussed.

2. Theory

The carbon-13 relaxation in methylene group (AMX or AX_2 spin system) is usually dominated by the pairwise dipole–dipole interaction between the carbon nucleus and the two protons. At high magnetic fields, the chemical shielding anisotropy (CSA) can also act as a source of relaxation, in particular for the cross-correlated relaxation rates.

The longitudinal relaxation in a multiple-spin system is conveniently described in terms of magnetization modes, v, and the relaxation superoperator, Γ [7,34]:

$$\mathrm{d}v(t)/dt = -\Gamma\Delta v \tag{1}$$

where Δv indicates deviation of the expectation values from equilibrium. The expanded form of Eq. (1) and a similar equation of motion related to transverse relaxation were provided in our previous article [21].

Under certain conditions, the relaxation equations can be simplified. The "standard" relaxation parameters, T_1^{-1}, T_2^{-1} and NOE factor $(1+\eta)$ can then be expressed as [29]:

$$T_{1\mathrm{DD}}^{-1} = (n_\mathrm{H}/4)\{J_\mathrm{CH}(\omega_\mathrm{H}-\omega_\mathrm{C}) + 3J_\mathrm{CH}(\omega_\mathrm{C}) + 6J_\mathrm{CH}(\omega_\mathrm{H}+\omega_\mathrm{C})\} \tag{2}$$

$$T_{2\mathrm{DD}}^{-1} = T_{1\rho\mathrm{DD}}^{-1} = (n_\mathrm{H}/8)\{4J_\mathrm{CH}(0) + J_\mathrm{CH}(\omega_\mathrm{H}-\omega_\mathrm{C}) + 3J_\mathrm{CH}(\omega_\mathrm{C}) + 6J_\mathrm{CH}(\omega_\mathrm{H}) + 6J_\mathrm{CH}(\omega_\mathrm{H}+\omega_\mathrm{C})\} \tag{3}$$

$$\eta = (\gamma_\mathrm{H}/\gamma_\mathrm{C})\frac{6J_\mathrm{CH}(\omega_\mathrm{H}+\omega_\mathrm{C}) - J_\mathrm{CH}(\omega_\mathrm{H}-\omega_\mathrm{C})}{J_\mathrm{CH}(\omega_\mathrm{H}-\omega_\mathrm{C}) + 3J_\mathrm{CH}(\omega_\mathrm{C}) + 6J_\mathrm{CH}(\omega_\mathrm{H}+\omega_\mathrm{C})} \tag{4}$$

where n_H is the number of protons directly bonded to the carbon ($n_\mathrm{H}=2$ for a methylene group), and $J_\mathrm{CH}(\omega)$ is the carbon–proton dipolar auto-correlation spectral density function, evaluated at combinations of carbon-13 and proton Larmor frequencies. Other mechanisms than dipole–dipole (DD) interaction are neglected in the case of auto-correlated relaxation (*vide infra*).

The transfer of longitudinal carbon-Zeeman order into the three-spin order and the corresponding transfer under carbon-spin-lock conditions are described by two cross-correlated dipolar relaxation rates. These two types of CCRRs are related to dynamic parameters via spectral densities according to [5,14,29,35]:

$$\Gamma_{ab}^{\text{long}} = 2J_{ab}(\omega_\mathrm{C}) \tag{5}$$

$$\Gamma_{ab}^{\text{spin-lock}} = \frac{4}{3}J_{ab}(\omega_1) + J_{ab}(\omega_C) \approx \frac{4}{3}J_{ab}(0) + J_{ab}(\omega_C) \tag{6}$$

where ω_1 is the strength of the spin-lock field, expressed in the angular frequency units. This quantity is much smaller than the Larmor frequencies, which motivates the approximate equality in the last part of Eq. (6). Following Daragan [36], we consider the motion of two vectors a and b, which can be defined as unit vectors directed along the CH bond in the case of dipolar relaxation. In the case of transfer between the Zeeman order and the longitudinal two-spin order (and corresponding processes under spin-lock conditions), we encounter dipolar-CSA cross-correlated relaxation rates. These involve analogous expressions with one of the vectors directed along the principal axis of the CSA tensor, assumed to be of axial symmetry. When $a \neq b$, $J_{ab}(\omega) = J_{\mathrm{CH,CH'}}(\omega)$ or $J_{\mathrm{CH,C}}(\omega)$ represent cross-correlated spectral density for interference between the two dipolar interactions and a dipolar interaction and CSA, respectively.

The next issue to consider is the form of the spectral densities. This depends on the model we choose. The simplest model treats γ-CD as a rigid spherical molecule reorienting isotropically in its environment by small-step rotational diffusion. In this simple approach, called the spherical top model, we have only one dynamical parameter (one rotational correlation time τ_M) and the spectral densities have the following form: [21,29,37].

$$J_a(\omega) = (2/5)\xi_{\mathrm{CH}}^{\mathrm{DD2}}\frac{\tau_\mathrm{M}}{1+\omega^2\tau_\mathrm{M}^2} \tag{7}$$

$$J_{ab}(\omega) = (3/10)\xi_{\mathrm{CH}}^{\mathrm{DD}}\xi_{\mathrm{CH'}}^{\mathrm{DD}}(1/2)(3\cos^2\Theta_{ab}-1)\left(\frac{\tau_\mathrm{M}}{1+\omega^2\tau_\mathrm{M}^2}\right) \tag{8}$$

where $\xi_{\mathrm{IS}}^{\mathrm{DD}} = \left(\frac{\mu_0}{4\pi}\right)\left(\frac{\gamma_I\gamma_S\hbar}{r_{\mathrm{IS}}^3}\right)$ is the dipolar coupling constant (DCC), μ_0 is the permeability of a vacuum, ħ is the Planck's constant, τ_M is the unique rotational correlation time, r_{IS} is the distance between two spins and Θ_{ab} denotes the angle between the principal axes of the two interactions (here, $\Theta_{\mathrm{CH,\,CH'}}$ is the angle between the two dipolar vectors CH and CH′). Given the cylindrical (rather than spherical) symmetry of the molecule, it might be more appropriate to treat γ-CD as a symmetric top. However, inspection of the relaxation data in the previous carbon-13 relaxation study of cyclodextrins from our laboratory does not motivate this complication [23].

A rigid molecule treatment of carbohydrates is in general not a good approximation, as some internal motions influence both the endocyclic carbons of methine groups and the exocyclic carbons of the methylene groups. In earlier work on carbohydrates from our laboratory, we have commonly used the Lipari–Szabo model free approach [32,33] for analyzing the data for both the CH and CH_2 groups [25,38,39]. The spectral density function is obtained by considering two types of motions, a rapid local motion and a slower global motion. The auto- and cross-correlated spectral density functions in this model are [40]:

$$J_a(\omega) = (2/5)\xi_{\mathrm{CH}}^{\mathrm{DD2}}\left(\frac{S_{\mathrm{CH}}^2\tau_\mathrm{M}}{1+\omega^2\tau_\mathrm{M}^2} + \frac{\left(1-S_{\mathrm{CH}}^2\right)\tau}{1+\omega^2\tau^2}\right) \tag{9}$$

$$J_{ab}(\omega) = (3/10)\xi_{\mathrm{CH}}^{\mathrm{DD}}\xi_{\mathrm{CH'}}^{\mathrm{DD}}(1/2)(3\cos^2\Theta_{ab}-1) \times\left(\frac{S_{\mathrm{CH}}S_{\mathrm{CH'}}\tau_\mathrm{M}}{1+\omega^2\tau_\mathrm{M}^2} + \frac{(1-S_{\mathrm{CH}}S_{\mathrm{CH'}})\tau}{1+\omega^2\tau^2}\right) \tag{10}$$

Here, the overall reorientation of the molecule is described by a global correlation time, τ_M, and the local fast motion is characterized by a local correlation time τ_e and auto- and cross-correlation order parameter S_{CH}^2 and $S_{\mathrm{CH}}S_{\mathrm{CH'}}$, which reflects the spatial restriction of the local motion. The symbol τ is related to the correlation times by: $\tau^{-1} = \tau_\mathrm{M}^{-1} + \tau_\mathrm{e}^{-1}$.

If the generalized order parameter is high, the global correlation time is not too long and the local correlation time is short, then the second term in the parentheses in Eqs. (9) and (10) can be neglected. We then talk about the truncated Lipari–Szabo model. The truncated Lipari–Szabo model is fully equivalent to the "rigid body with DCC scaling" approach, where one uses Eqs. (7) and

(8) but allows the DCC to attain a reduced value. The spherical top model with scaling of the DCC (or of the effective carbon-proton distance) has been applied in a study of hexamethylene tetramine (HMTA) [37]. The scaled distance came out somewhat longer than the equilibrium bond length, which was possible to explain in terms of vibrational averaging effects. This approach to dipolar relaxation has also been found useful by other authors [21,24].

Another dynamic model of interest in the present work describes a specific motional process in terms of random jumps. This model allows a simple description of local conformational changes, an important issue in structural and dynamical NMR studies of γ-cyclodextrin where we deal with the conformational dynamics of the hydroxymethyl group (the ω-torsion). One of the goals of the present paper is to investigate in which way the cross-correlated relaxation measurements can provide new information on that topic. The three different staggered conformations of the cyclodextrin are illustrated in Fig. 1.

One can in principle consider the conformational exchange process as a three-site or a two-site jump. Using earlier evidence [25,41,42], the two-site jump seems to be a better choice. The use of jump models to probe the local dynamic and conformational motion in methylene groups has been discussed by Ernst and Ernst and by Daragan et al. [14,36]. Considering an internal motion and an overall isotropic rotation, the spectral densities for the two-site jump model take the form:

$$J_{ab}(\omega) = C\xi_a\xi_b \sum_m a_m^{ab} J_m(\omega) \tag{11}$$

$$J_m(\omega) = \left[1 - 4P(1-P)\sin^2(m\gamma_j)\right]\tau_M/\left(1+(\tau_M\omega)^2\right) + 4P(1-P)\sin^2(m\gamma_j)\tau'/\left(1+(\tau'\omega)^2\right) \tag{12}$$

The constant C is equal to (2/5) for auto and (3/10) for cross-correlated spectral densities, ξ_i is the relevant interaction strength, the symbol τ' represents $\tau'^{-1} = \tau_M^{-1} + \tau_j^{-1}$, where τ_M is the global correlation time, τ_j is the jump correlation time (inverse jump rate) [36], P is the population of one of the rotamers, γ_j is the jump half-angle (the jump occurs between $+\gamma_j$ and $-\gamma_j$) and the coefficients a_m^{ab}, with $m = 0,1,2$, can be expressed as follows:

$$\begin{aligned} a_0^{ab} &= P_2(\cos\theta_a)P_2(\cos\theta_b) \\ a_1^{ab} &= 3\cos\theta_a\cos\theta_b\sin\theta_a\sin\theta_b\cos(\phi_a-\phi_b) \\ a_2^{ab} &= (3/4)\sin^2\theta_a\sin^2\theta_b\cos(2\phi_a-2\phi_b) \end{aligned} \tag{13}$$

$P_2(x) = 1/2(3x^2-1)$ is the second order Legendre polynomial. The angles θ_a and θ_b are the polar angles (angles which vectors a and b make with the jump axis) and $(\phi_a - \phi_b)$ is the angle between the projections of the principal axes of the two interactions on the plane perpendicular to the jump axis (C_5–C_6 bond in the case of γ-CD). We can take advantage of the following property of coefficients a_m^{ab} to determine Θ_{ab} for comparison with other models:

$$a_0^{ab} + a_1^{ab} + a_2^{ab} = P_2(\cos\Theta_{ab}) \tag{14}$$

The angles θ_a and θ_b should not be confused with the Θ_{ab} angle between the two principal axes, introduced in Eq. (8).

In both the Lipari–Szabo and the two-site jump models, one considers two types of motion. We propose here a generalization of the two-site jump model, which in a simplified way includes *three* types of motion: the global reorientation, the conformational two-site jumps of the hydroxymethyl group and a rapid local motion averaging down (scaling down) the dipole–dipole interaction. The three motions are assumed to be statistically independent. The rapid local motion refers to vibrations/librations and is assumed to follow the same assumptions as those leading to the truncated Lipari–Szabo model or to the spherical rigid rotor with DCC scaling. The interesting conformational exchange process is treated explicitly as a jump process, which can in principle occur on the time scale similar to that of the overall reorientation. This model yields the spectral density expressions in Eqs. ((11)–(14)), but now allowing the dipolar coupling constants to be reduced in magnitude by the rapid local motions.

It is worthwhile to mention here that, in addition to the primary ^{13}C spin relaxation mechanism (the dipole interaction with its bonded proton), the influence of CSA on spin dynamics cannot be neglected at high magnetic fields, especially in the case of cross-correlated relaxation rates. For the DD/CSA cross-correlated interaction, the second interfering mechanism is CSA and the cross-correlated spectral density in Eq. (13) takes the following form:

$$J_{ab}(\omega) = -(4/5)\xi_{CH}^{DD}\xi_C^{CSA}\sum_m a_m^{ab}J_m(\omega) \tag{15}$$

All parameters have the same definition as in Eqs. ((11)–(14)), the only difference is replacing one dipolar coupling constant by the CSA interaction strength. The symbol Θ_{ab} denotes here the angle between the CH dipole and the principal axes of CSA tensor for the DD/CSA cross-correlated relaxation. The coefficient $\xi_C^{CSA} = \omega_C\Delta\sigma$ is the CSA interaction strength. We shall come back to the definition of $\Delta\sigma$ later in the discussion section.

3. Experimental

NMR experiments were performed on a sample of 77 mM solution of γ-cyclodextrin in a 7:3 molar ratio mixture of D_2O and DMSO-d_6. The solvents D_2O and DMSO-d_6, obtained from Cambridge Isotope Laboratories, Inc., and γ-cyclodextrin provided by Fluka, were used without further purification. The solution was transferred to a 5-mm and a 10-mm NMR tube and sealed under vacuum after removing the dissolved gas using repeatedly ultrasonic bath and mild evacuation. The 10-mm tube sample was used for CCRR measurements at 9.4 and 14.1 T, while the conventional relaxation experiments at these fields and all measurements at 21.1 Tesla were performed on the 5-mm sample.

The experiments were carried out at two temperatures, 50 and 70 °C, and three magnetic fields. Experiments at 9.4 T were performed on a Bruker Avance 400 spectrometer, equipped with broadband (BBO) 5-mm and 10-mm probeheads. A Varian Inova 600 spectrometer equipped with a 5-mm HCX and a 10-mm broadband probehead was used to carry out experiments at 14.1 Tesla. Measurements at 21.1 Tesla were performed on a Bruker Avance 900 instrument, equipped with a TCI cryoprobe. The sample temperature was calibrated carefully using methanol or ethylene glycol chemical shift thermometers [43], while the temperature was regulated by means of the standard variable temperature controllers provided by the instrument manufacturers.

The carbon-13 spin-lattice relaxation time (T_1) was measured under proton decoupling, using the inversion-recovery method with 10–12 different delays. The spin-lattice relaxation time in the rotating frame ($T_{1\rho}$) was measured with the spin-lock field strength of 3.7 kHz at the two lower fields, while 1 kHz was employed at 21.1 Tesla. In all cases, the carbon carrier frequency was set close to resonance. We have taken advantage of the fact that, in the absence of chemical exchange on the microsecond timescale, $T_{1\rho}$ is equivalent to T_2 [44,45]. The nuclear Overhauser

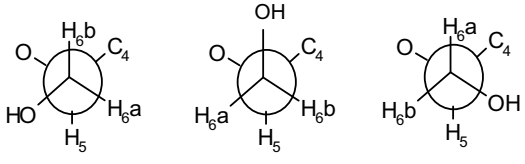

Fig. 1. Rotamers in cyclodextrins around the C5–C6 axis.

enhancements (NOE) were determined using the dynamic NOE (DNOE) technique described previously [21,46]. The recycle delay of about five times the longest T_1 was used in the inversion-recovery and spin-lock experiments, while it was about $10T_1$ in the NOE experiments. Broadband proton decoupling during acquisition was performed using the Waltz-16 scheme, with a typical decoupler 90° pulse duration of about 100 μs. The line broadening of 3–5 Hz was applied before evaluating line intensities. The three-parameter and the two-parameter exponential fitting routines provided by the instrument manufacturers were used for evaluating the spin-lattice relaxation rate and $T_{1\rho}$ respectively. The carbon-13 90° pulse duration was about 7 μs (5 mm probe) and about 15 μs (10 mm probe) at 9.4 Tesla; the corresponding values were 13 and 15 μs at 14.1 T, while the carbon-13 90° pulse duration on the TCI probe at 21.1 T was about 12 μs. The spectral width was typically around 60 ppm; the acquisition time was 1.2 s and the number of transients 128–512 at the two lower fields. At 21.1 T, the acquisition time was 0.2 s and the number of scan was 32–64. The accuracy of the T_1, $T_{1\rho}$ and NOE data is estimated to be better than 3, 5 and 5%, respectively. All the experiments were repeated at least twice and average values are reported.

The nuclear spin relaxation rates associated with cross-correlated dipole–dipole interactions were measured using the simple method explained in our previous article [21]. For the longitudinal case, we used the simple carbon-13 inversion-recovery experiment without proton decoupling [6,14,16,47–49]. For the CCRR experiments, a 10 Hz line broadening was used. Selected traces from proton-coupled inversion recovery experiment on γ-CD are demonstrated in Fig. 2. It is obvious from the spectra that the three lines relax with different rates. As noted previously, the dipolar cross-correlation spectral densities can be derived from standard proton-coupled ^{13}C inversion-recovery NMR relaxation experiments [7,16,36] by measuring initial relaxation rates for the inner (W_i) and outer (W_o, average value for left and right) lines of the methylene group triplet as defined by following equation:

$$\Gamma^{DD/DD}_{CH,\,CH'} = (1/2)(W_o - W_i) \quad \text{where } W_o = (1/2)(W^L_o + W^R_o) \tag{16}$$

Relaxation delays were chosen from some ms to about half T_1. In addition, one long delay was included to provide a reference spectrum. The number of transient was about 2000 (at 9.4 and 14.1 T), while 512 scans were sufficient in order to provide excellent signal-to-noise ratio using the cryo-probe at 21.1 T. Other experimental parameters were the same as in the proton-decoupled T_1 measurements.

Fig. 3 shows selected traces from proton coupled spin-lock experiment on γ-CD. In analogy with the case of the longitudinal relaxation, the transverse relaxation was studied by simple spin-lock experiments in the presence of spin–spin couplings. After an initial 90° carbon-13 pulse, the transmitter phase was switched by 90° and a long, weak ($\gamma B_1/2\pi \approx 3$ kHz at the lower two fields, ≈1 kHz at 21.1 Tesla) carbon-13 pulse of variable length, τ, followed. During the τ delay, the transverse cross-correlated relaxation process transferred some of the transverse magnetization into the double antiphase term. Subsequent detection of the FID and the Fourier transformation resulted in spectra displaying τ – dependent multiplet asymmetries.

As it is obvious from the spectra in Figs. 2 and 3, also the two outer lines relax at different rates: the right outer line relaxes faster than the left one. The cross-correlation between the carbon-hydrogen dipolar interaction and the carbon CSA tensor is responsible for this difference [36]. The longitudinal and transverse DD/CSA cross-correlated rate constants were determined from the same proton-coupled carbon-13 inversion-recovery and spin lock experiments, using the difference between the initial relaxation rates of two outer lines of the ^{13}C multiplet and employing the following equation [15,16,36]:

$$\Gamma^{DD/CSA}_{CH,\,C} = (1/2)(W^L_o - W^R_o) \tag{17}$$

All the least-squares fits were performed using MATLAB routines written in-house.

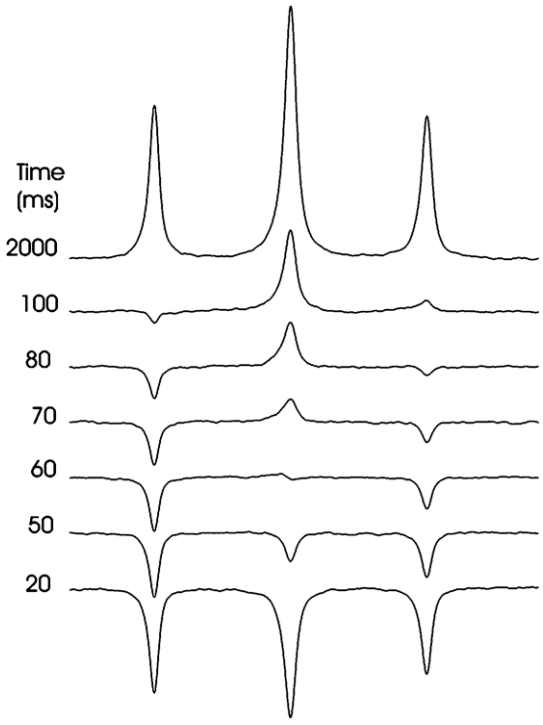

Fig. 2. Selected traces from the proton coupled ^{13}C inversion- recovery experiment on γ-CD.

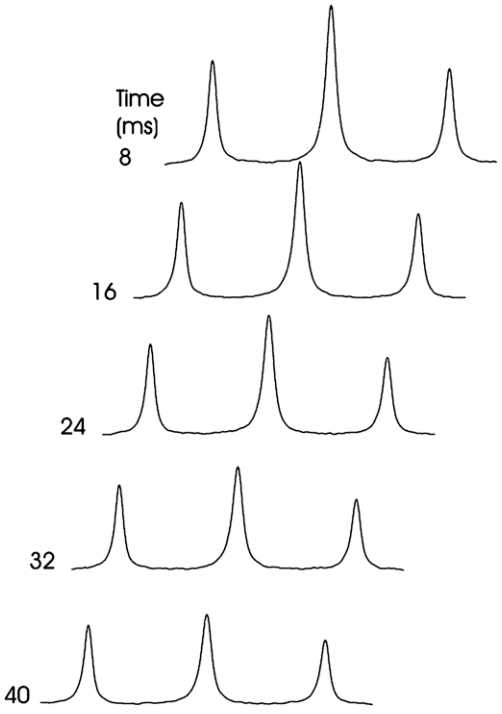

Fig. 3. Selected traces from the proton coupled ^{13}C spin-lock experiment on γ-CD.

4. Results and discussion

The measurements for hydroxymethyl group as well as for the ring methine carbons were carried out at three fields (9.4, 14.1 and 21.1 T) and two temperatures (323 and 343 K). The elevated temperatures were chosen in order to limit the width of the resonance lines. The experimental "conventional" relaxation parameters for the methine carbons are listed in Table 1.

The small NOE ($1+\eta$ less than 3) and unequal (and field-dependent) T_1^{-1} and T_2^{-1} demonstrate that the measurements are outside the extreme narrowing regime for γ-CD at both temperatures, which is reasonable given the size of an eight residue sugar and the use of a relatively viscous solvent mixture. The frequency-dependent relaxation data can thus be interpreted quantitatively by employing Eqs. (2)–(4), together with an appropriate dynamic model. Table 2 summarizes the conventional ^{13}C relaxation parameters (T_1^{-1}, T_2^{-1}, NOE) and the cross-correlated relaxation rates, $\Gamma^{\text{long}}_{\text{CH, CH}'}$, $\Gamma^{\text{spin-lock}}_{\text{CH, CH}'}$, $\Gamma^{\text{long}}_{\text{CH, C}}$ and $\Gamma^{\text{spin-lock}}_{\text{CH, C}}$ for the methylene carbon.

To characterize the solution state dynamics of γ-CD, the experimental data for methine carbons were first fitted using the spherical top model with adjustable DCC, equivalent to the truncated Lipari–Szabo approach. All ring carbons were considered as dynamically equivalent [23]. The results from these least-square fittings are collected in Table 3 (fit a). Uncertainties estimated by a Monte Carlo procedure are represented by the numbers in parentheses. Reasonable overall correlation times of 1.6 ns (at 323 K) and 0.9 ns (at 343 K) and a CH distance of 113 pm were obtained. This τ_M was also used as an initial point for fitting the methylene group data using the two-site jump model. We shall come back to this point later.

The Lipari–Szabo approach was also applied to the conventional methine carbon relaxation data to obtain the overall correlation time τ_M, the order parameter S^2 and the fast local internal correlation time τ_e (fitting results in Table 3 (b). A dipolar coupling constant of 22.8 kHz corresponding to a fixed CH distance (r_{CH} = 1.098 Å) was used. The value of τ_M equal to 1.7 ns obtained from Lipari–Szabo approach and 1.6 ns from isotropic model with DCC scaling at 323 K are in good agreement with each other and seems to be reasonable in comparison to the 1.23 ns at 322 K obtained in Kowalewski and Widmalm [23], by taking into account the higher concentration of γ-CD in the present work. The order parameter S^2 = 0.82 ± 0.04 at 323 K for the ring carbons is also close to the previously reported value S^2 = 0.81 ± 0.01at 322 K. Table 3 includes also the results from similar fitting procedures for the methylene group. Both kinds of fitting yield here a shorter overall correlation time than for the methine moieties, which again is in agreement with earlier work [23]. In addition, the Lipari–Szabo fitting gives a smaller order parameter, while the isotropic reorientation model results in a longer effective CH distance (or in a lower dipolar coupling constant, ξ^{DD}_{IS}). The CH distance obtained in this case is even longer than the effective internuclear distance for the methylene groups in HMTA molecule (r_{CH} = 114.2 pm) [37]. The overall correlation times determined by both models are in agreement within the range of error. The temperature dependence of τ_M and τ_e is in all cases reasonable, both correlation times decrease with increasing temperature. However, the uncertainties in τ_e are large in all cases, as usually observed [25,39].

The emphasis in the present work is on the use of the dipolar CCRR data, along with the conventional relaxation parameters. In the first step of the analysis, we have thus investigated the effects of including the dipolar CCRRs in the above-mentioned fitting procedures for the methylene group. We used the Lipari–Szabo model and optimized simultaneously four parameters: τ_M, S^2, τ_e and $\Theta_{CHCH'}$. We performed also a three parameter (τ_M, $\Theta_{CHCH'}$ and r_{CH}) fitting, while using the isotropic reorientation with DCC scaling model. The results from these least-squares fittings are gathered in Table 4 (fit a and b). The correlation times and order-parameters agree with the results from the fitting without CCRRs (fit a and b for the methylene group in Table 3), in most cases within the range of Monte Carlo errors, demonstrating the consistency of the conventional relaxation data and the CCRRs. An additional structural parameter, $\Theta_{CHCH'}$, the angle between the two dipolar interactions, was also determined. The angle $\Theta_{CHCH'}$ of about 115° deviates somewhat from the tetrahedral angle, 109.5°, which may indicate the effect of internal motion. The analysis of the CCRRs in the

Table 1
Relaxation parameters for ring carbons in γ-cyclodextrin, all rates are in s^{-1}

Magnetic field (T)	9.4		14.1		21.1	
Temperature (K)	323	343	323	343	323	343
T_1^{-1}	4.68	4.76	2.91	3.29	1.72	2.17
T_2^{-1}	8.97	6.50	7.87	5.03	-	-
$1+\eta$	1.35	1.49	1.31	1.41	1.26	1.28

Table 2
Relaxation parameters for methylene group carbons in γ-cyclodextrin, all rates are in s^{-1}

Magnetic field (T)	9.4		14.1		21.1	
Temperature (K)	323	343	323	343	323	343
T_1^{-1}	8.10	7.46	5.33	5.44	3.18	3.65
T_2^{-1}	13.33	9.33	11.76	7.68	9.02	6.46
$1+\eta$	1.43	1.63	1.33	1.51	1.25	1.33
$\Gamma^{\text{long}}_{\text{CH, CH}'}$	−1.98	−1.58	−1.27	−1.19	−0.72	−0.83
$\Gamma^{\text{spin-lock}}_{\text{CH, CH}'}$	−3.55	−2.16	−3.34	−1.87	−2.79	−1.71
$\Gamma^{\text{long}}_{\text{CH, C}}$	−0.72	−0.64	−0.74	−0.71	−0.65	−0.75
$\Gamma^{\text{spin-lock}}_{\text{CH, C}}$	−1.47	−0.71	−2.38	−0.85	−2.74	−1.63

Table 3
Least-squares fitting of conventional relaxation data for methine and methylene groups

	Methine		Methylene	
Temperature (K)	323	343	323	343
(a) Isotropic reorientation with DCC scaling				
τ_M(ns)	1.61(0.1)	0.87(0.07)	1.27(0.04)	0.73(0.10)
r_{CH}(pm)	112.4(0.6)	113(0.5)	116(0.3)	117(1)
SD	4.4	3.1	5.3	2.4
(b) Lipari–Szabo model free approach				
τ_M(ns)	1.69(0.08)	0.91(0.09)	1.32 (0.08)	0.78(0.09)
τ_e(ps)	30(29)	7(44)	11(17)	9(22)
S^2	0.84(0.02)	0.78(0.05)	0.70(0.03)	0.62(0.05)
SD	7.6	5.5	7.9	4.6

Standard deviation (SD) is in percent.

Table 4
Results of least-squares fitting for the methylene group, including the dipolar CCRRs, we assume that for auto-relaxation $S^2_{CH} = S_{CH}S_{CH'}$

(a) Lipari–Szabo model free approach					
T (K)	τ_M (ns)	τ_e (ps)	$S_{CH}S_{CH'}$	$\Theta_{CHCH'}$	SD
323	1.42(0.04)	14(13)	0.69(0.02)	115(0.3)	6.2
343	0.82(0.04)	16(19)	0.64(0.04)	115(0.4)	5.0
(b) Isotropic reorientation with DCC scaling					
T(K)	τ_M (ns)	r_{CH} (pm)	—	$\Theta_{CHCH'}$	SD
323	1.37(0.06)	116(0.3)	—	116(0.5)	5.9
343	0.78(0.03)	117(0.5)	—	115(0.2)	2.8

$\Theta_{CHCH'}$ is in degrees, SD in percent.

CH_2 groups in HMTA led also to the angle between the principal axes of the two interactions somewhat larger than the tetrahedral angle [21,37].

Next, we report the fittings (including and excluding the dipolar CCRRs) to what we believe is a more realistic model, including two-site jumps and the DCC scaling, Eqs. ((11)–(14)). As noted in the theory section, this model may be expected suitable for investigating the conformational motion of the hydroxymethyl group. Some more parameters enter the model, and all of them are not fully independent of each other in the statistical sense. Therefore, we use throughout fixed values of the polar angles θ_a and θ_b, set to the tetrahedral values, 70.5°. Even with these assumptions, performing simultaneous fitting of all the remaining parameters is not without problems. We have therefore decided to perform the analysis in steps. The fitting strategy was very similar for the data including and excluding the CCRRs. First, we have assumed an "ideal" two-site jump angle $\gamma_j = 60°$ and used the overall correlation time τ_M from the isotropic rotor with DCC scaling fitting for the methine carbons. The fitted values of the inverse jump rate, τ_j, the effective CH distance, r_{CH}, and the population P are shown in Table 5, entries a (without CCRRs) and b (with CCRRs). For the case when the CCRRs were included, the fitting also yielded $(\phi_a - \phi_b)$. For given values of θ_a,θ_b, and $(\phi_a - \phi_b)$, the angle between the two dipolar interactions $\Theta_{CHCH'}$ can be obtained from Eq. (14). We list this latter angle in Table 5, in order to facilitate comparison with Table 4.

Using these values as a starting point, we then applied a step-by-step adjustment of one of the parameters (γ_j, τ_M) at a time, together with τ_j, r_{CH} and P (as well as $(\phi_a - \phi_b)$ if the CCRRs were included). Table 5 contains the result obtained in this procedure. Indices "c" and "e" refer to a set of parameters resulting from only the conventional relaxation data and the parameter set denoted by index "d" and "f" correspond to the relaxation data set including the DD/DD CCRRs. Finally, we have also fitted all parameters in the Table, indices "g" and "h".

The first observation we make has to do with the structural parameters, r_{CH} and $\Theta_{CHCH'}$. These seem to be rather stable throughout Table 5. Looking then at the fits with the overall rotational correlation times fixed at the values from the methine carbons (fits a–d), we find that they work moderately well. The most interesting parameter of the model, the inverse jump rate for the hydroxymethyl group, is estimated to fall in the sub-nanosecond range, somewhat shorter than the estimates based on ultrasonic relaxation studies of monosaccharides [50,51]. Including the CCRRs in the fit (cases b and d) results, at both temperatures, in somewhat smaller values of τ_j. Allowing for adjustment of the jump angle (compare pairwise a and c or b and d) seems to have a very small effect on the jump rates (again at both temperatures), it appears that the variations in the jump angle and the populations compensate each other.

The fits e – h are interesting. The quality of these fits, expressed as the standard deviations of the dependent variable (last column of the table), is generally better than for the a–d fits. In particular the data at 343 K yields quite small standard deviations. For the 343 K data, allowing adjustment of the overall rotational correlation time leads to stable results for τ_M, reduced by about 10% compared to the methine carbon values, which is gratifying. The fitted τ_j values depend on whether the CCRRs are included or not, but not on whether the jump angle is fixed or not. In a sense, this again is encouraging, as it is consistent with our earlier monosaccharide study [25], where we observed that the CCRRs seemed to be a sensitive measure of the jump processes in a hydroxymethylene moiety. It is also worth pointing out that the uncertainties in the fitted τ_j, from the Monte Carlo analysis, are very large if the CCRRs are omitted and attain more acceptable (though still large) values when the CCRRs are included. For the 323 K data, allowing adjustment of the overall rotational correlation time leads to quite different results for τ_M (as well as for τ_j), depending on whether the CCRRs are included or not. On the other hand, locking the jump angle or treating it as an adjustable parameter (compare pairwise fits 323e and g, 323f and h) does not seem to be important in that case either. The jump times obtained at both temperatures in fits f or h are significantly shorter than the values proposed based on ultrasonic relaxation in monosaccharides. On the other hand, according to the preliminary analysis of trajectories from a 30 ns classical MD simulation for α-cyclodextrin (CSFF force field) in SPCE water, the jump rate might be as high as about 15 ns^{-1} (Arnold Maliniak and Kevin Naidoo, private communication).

At both temperatures, we can notice that the most advanced fits h produce unrealistically small jump angles. Fits f, with the jump angle locked at 60°, produce on the other hand a rather unbalanced distribution of populations between the two sites, but this is perhaps easier to accept on physical grounds (we note that a 20:1 population ratio corresponds, according to the Boltzmann distribution, to an energy difference of about 8 kJ mol^{-1}). Pursuing the energetics discussion further and assuming that the rates corresponding to the fits f and h at the two temperatures are correct, we can estimate the activation energy of about 40 kJ mol^{-1} for the jump process; none of these two energy values seems unreasonable. Thus,

Table 5
Least-square fitting for the methylene group using the two-site jump model

T (K)/fit	τ_M (ns)	τ_j (ns)	γ_j	$\Theta_{CHCH'}$	r_{CH} (pm)	P	*SD*
323a	1.61	0.91(0.16)	60	–	115.6(0.2)	0.15(0.01)	4.8
323b	1.61	0.64(0.13)	60	110.0(0.5)	115.4(0.2)	0.11(0.01)	7.0
323c	1.61	0.91(0.16)	24(1)	–	114.6(1.5)	0.37(0.08)	4.2
323d	1.61	0.66(0.14)	23(15)	110.2(0.6)	115.4(0.2)	0.50(0.03)	6.8
323e	2.41(0.30)	1.24(0.15)	60	–	115.8(0.2)	0.50(0.14)	4.5
323f	1.44(0.06)	0.33(0.15)	60	110.2(0.5)	115.3(0.3)	0.06(0.02)	7.4
323g	2.38(0.32)	1.24(0.17)	48(2.4)	–	115.8(0.2)	0.50(0.15)	4.4
323h	1.45(0.06)	0.38(0.18)	17(12)	110.2(0.6)	115.2(0.6)	0.51(0.06)	6.3
343a	0.87	0.92(0.68)	60	–	116.5(0.4)	0.17(0.10)	5.5
343b	0.87	0.40(0.22)	60	109.8(1.4)	116.2(0.9)	0.06(0.02)	5.9
343c	0.87	0.81(0.57)	35(4)	–	116.3(1.3)	0.18(0.09)	6.0
343d	0.87	0.42(0.25)	21(16)	109.9(0.6)	116.3 (0.4)	0.50(0.08)	5.2
343e	0.81(0.09)	0.22(0.28)	60	–	113.1(6.4)	0.15 (0.18)	2.1
343f	0.80(0.03)	0.14(0.09)	60	109.4(2.6)	115.2(2.0)	0.07(0.04)	2.8
343g	0.81(0.11)	0.21(0.27)	69(11)	–	112.9(6.9)	0.20(0.20)	4.2
343h	0.80(0.03)	0.15(0.08)	16(11)	109.5(3.0)	115.5(1.7)	0.50(0.11)	2.0

(a) τ_M from methine carbons, jump angle 60°, only conventional relaxation data. (b) τ_M from methine carbons, jump angle 60°, the CCRR data included. (c) τ_M from methine carbons, only conventional relaxation data. (d) τ_M from methine carbons, the CCRR data included. (e) Jump angle 60°, only conventional relaxation data. (f) Jump angle 60°, the CCRR data included. (g) All parameters adjusted, only conventional relaxation data. (h) All parameters adjusted, the CCRR data included.
Angles are in degrees, SD in percent.

the tentative conclusion based on Table 5 is that we find the fit f probably most trustworthy. The calculated field-dependences of all the relaxation rates, using the parameters of the fits f in Table 5 are shown, together with the experimental data, in Fig. 4.

Additional two relaxation observables, the longitudinal and transverse dipolar-CSA CCRRs, $\Gamma^{DD/CSA}_{CH,C}$, were determined from the coupled inversion-recovery and spin-lock experiments as explained in experimental section. They are shown as $\Gamma^{long}_{CH,C}$ and $\Gamma^{spin-lock}_{CH,C}$, respectively, in Table 2. Similar measurements for a CH_2 group have earlier been reported by Chenon and Werbelow [13]. Following their approach, we did not use the DD/CSA cross-correlated relaxation rates in our analysis to determine the dynamics. On the other hand, making use of the dynamical information from the dipolar relaxation, we estimated the CSA parameters from these relaxation data.

The longitudinal and transverse DD/CSA CCRRs obtained from Eq. (17) are related to dynamical parameters by means of spectral densities according to Eqs. (5) and (6). The cross-correlated spectral densities $J_{CH,C}$ refer to the interference between the CH dipolar interaction and the carbon-13 CSA tensor. According to Daragan and Mayo [15,36], the spectral densities have the form of Eq. (15). The shielding anisotropy, $\Delta\sigma$, is normally defined as $\Delta\sigma = \sigma_\perp - \sigma_\parallel = \sigma_{zz} - (\sigma_{xx} + \sigma_{yy})/2$, with $|\sigma_{zz} - \sigma_{iso}| > |\sigma_{xx} - \sigma_{iso}| > |\sigma_{yy} - \sigma_{iso}|$ and $\sigma_{iso} = 1/3(\sigma_{xx} + \sigma_{yy} + \sigma_{zz})$. We ignored the deviation

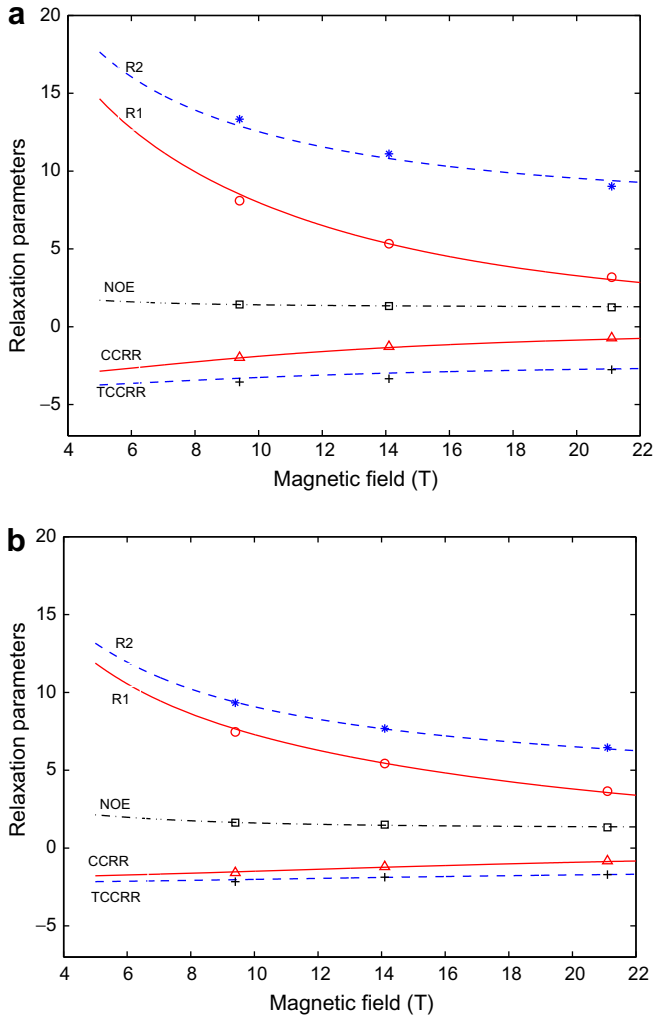

Fig. 4. Field dependence of calculated and experimental relaxation parameters at two temperatures. (a) 323 K, (b) 343 K. R1 = T_1^{-1}, R2 = T_2^{-1}, CCRR = $\Gamma^{long}_{CH,CH'}$, TCCRR = $\Gamma^{spin-lock}_{CH,CH'}$.

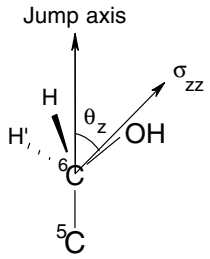

Fig. 5. Orientation of the carbon-13 CSA principal axis in the methylene group.

of chemical shielding tensor from axial symmetry to simplify the evaluation of CSA factor. It can be assumed that the principal component of CSA tensor σ_{zz} coincides with C_6–O bond (Fig. 5) and makes an angle θ_Z with the C5–C6 bond (the jump axis). Here, $\Theta_{ab} = \Theta_{CHC}$ is the angle between the principal axis of CSA tensor and the CH bond vector, while other parameters have the usual meaning, as explained in the theory section.

The DD/CSA CCRRs, listed in Table 2, were analyzed applying the two-site jump model. We fixed all dynamical parameters at the optimized values obtained from the conventional rates and DD/DD CCRRs (τ_M, τ_j, γ_j, r_{CH} and P from fit f in Table 5) and determined the $\Delta\sigma$. Since the three angles Θ_{CHC}, $\varphi_{CH} - \varphi_Z$ and θ_Z are interrelated, they were in the course of the fitting fixed at the tetrahedral values, and only $\Delta\sigma$ was adjusted. The values of $\Delta\sigma = 57.9 \pm 1.5$ at 323 K and $\Delta\sigma = 56.7 \pm 1.5$ at 343 K are in reasonable agreement with each other and in the range of the $\Delta\sigma$ value obtained for carbon-13 in other sugars [52–54]. The value of $\Delta\sigma$ is very sensitive to the value of θ_Z. When we consider a slightly different angle between the jump axis and the principal axis of the CSA tensor, *i.e.* $\theta_Z = 115°$, the fitting procedure results in the $\Delta\sigma = 50.6 \pm 1.2$ at 323 K and $\Delta\sigma = 44.0 \pm 1.2$ at 343 K.

Having estimated the CSA for the methylene carbon from the cross-correlated relaxation rates, we can now check the validity of the assumption that the non-dipolar mechanisms can be neglected for auto-correlated relaxation. We have estimated the CSA contributions to T_1^{-1} and T_2^{-1} for the methylene ^{13}C using the $\Delta\sigma$ values above and the Lipari–Szabo model. The highest CSA contribution to a relaxation rate (T_2^{-1} at 21 T and 323 K) was about 8% of the DD value. It is our opinion that this contribution is low enough to motivate the simplifying assumption that the non-dipolar mechanisms can be neglected. An alternative might be an iterative treatment of dynamics and CSA interaction strength, which we do not find reasonable.

5. Concluding remarks

Dipole–dipole cross-correlated relaxation rates, $\Gamma^{DD/DD}_{CH,CH'}$, in the methylene group provide possible structural tools as well as probes for conformational dynamics of hydroxymethyl groups in γ-cyclodextrin. We used the simple experimental schemes based on the initial rate technique to measure CCRRs. The experimental data were analyzed using different models. The standard or truncated Lipari–Szabo models allow a reasonable interpretation of the experimental data. We used also the experimental data sets to test a novel modification of the two-site jump model for the motion of the methylene group. We demonstrated that the modified two-site jump model has certain advantages over the Lipari–Szabo approach and the scaled isotropic reorientation model for interpreting relaxation data including the CCRRs. The auto- and cross-correlated relaxation data analyzes using two-site jump model including a scaled DCC or CH distance, yield a reasonably consistent picture of the dynamics. The analysis allows the estimation of conformer lifetimes of few hundreds of picoseconds, clearly

shorter than the correlation times for overall motion of the cyclodextrin.

Finally, we demonstrate that the dipolar-CSA CCRR, $\Gamma^{DD/CSA}_{CH,C}$, can be used to evaluate CSA parameters for the methylene group in γ-cyclodextrin. Because of the small value of CSA for the sugar carbons, its contribution to the "standard" relaxation is negligible, while the DD/CSA cross-correlation provides the possibility of estimation of CSA parameters in solution.

Acknowledgments

This work was supported by the Swedish Research Council and by Carl Tryggers Foundation for Scientific Research. We are indebted to the CERM infrastructure access program (EUNMR, contract RII3-026145) for the generous grant of the instrument time on the 21.1 T spectrometer, as well as for invaluable technical support. We are grateful to Professor Arnold Maliniak and Dr Baltzar Stevensson for valuable discussions.

References

[1] H. Shimizu, Theory of the dependence of nuclear magnetic relaxation on the absolute sign of spin-spin coupling constant, J. Chem. Phys. 40 (1964) 3357–3364.
[2] J.S. Blicharski, W. Nosel, Interference effect in nuclear magnetic relaxation for three-spin system, IV, Acta Phys. Pol. A 38 (1970) 25–32.
[3] J.S. Blicharski, Interference effect in nuclear magnetic relaxation, Acta Phys. Pol. 36 (1969) 211–218.
[4] M. Goldman, Interference effects in the relaxation of a pair of unlike spin-1/2 nuclei, J. Magn. Reson. 60 (1984) 437–452.
[5] A. Kumar, R.C.R. Grace, P.K. Madhu, Cross-correlations in NMR, Prog. Nucl. Magn. Reson. Spectrosc. 37 (2000) 191–319.
[6] D.M. Grant, C.L. Mayne, F. Liu, T.X. Xiang, Spin-lattice relaxation of coupled nuclear spins with applications to molecular motion in liquids, Chem. Rev. 91 (1991) 1591–1624.
[7] L.G. Werbelow, D.M. Grant, Intramolecular dipolar relaxation in multispin systems, Adv. Magn. Reson. 9 (1977) 189–299.
[8] D. Canet, Relaxation mechanism: magnetization modes, in: D.M. Grant, R.K. Harris (Eds.), Encyclopedia of Nuclear Magnetic Resonance, Wiley, Chichester, 1996, pp. 4046–4053.
[9] L.G. Werbelow, Relaxation Processes: Cross Correlation and Interference Terms, in: D.M. Grant, R.K. Harris (Eds.), Encyclopedia of Nuclear Magnetic Resonance, Wiley, Chichester, 1996, pp. 4072–4078.
[10] D. Frueh, Internal motions in proteins and interference effects in nuclear magnetic resonance, Prog. Nucl. Magn. Reson. Spectrosc. 41 (2002) 305–324.
[11] B. Brutscher, Principles and applications of cross-correlated relaxation in biomolecules, Concepts Magn. Reson. 12 (2000) 207–229.
[12] J. Cavanagh, W.J. Fairbrother, A.G. Palmer III, R. Mark, N.J. Skelton, Protein NMR Spectroscopy, 2nd ed., Academic Press, San Diego, 2007.
[13] M.T. Chenon, L.G. Werbelow, An NMR study of the solution dynamics of deltorphin-i, J. Am. Chem. Soc. 124 (2002) 14066–14074.
[14] M. Ernst, R.R. Ernst, Heteronuclear dipolar cross-correlated cross relaxation for the investigation of side-chain motions, J. Magn. Reson. A 110 (1994) 202–213.
[15] V.A. Daragan, K.H. Mayo, Asymmetric ^{13}C NMR multiplet relaxation and dipolar-CSA cross correlation for glycine ^{13}C-alphamethylenes in peptides, Chem. Phys. Lett. 206 (1993) 393–400.
[16] V.A. Daragan, M.A. Kloczewiak, K.H. Mayo, Carbon-13 nuclear magnetic resonance relaxation-derived Ψ, Φ bond rotational energy barriers and rotational restrictions for glycine $^{13}C\alpha$-methylenes in a GXX-repeat hexadecapeptide, Biochemistry 32 (1993) 10580–10590.
[17] J. Engelke, H. Ruterjans, Dynamics of β-CH and β-CH_2 groups of amino acid side chains in proteins, J. Biomol. NMR 11 (1998) 165–183.
[18] D. Yang, A. Mittermaier, Y.K. Mok, L.E. Kay, A study of protein side-chain dynamics from new ^{2}H auto-correlation and ^{13}C cross-correlation NMR experiments: application to the N-terminal SH_3 domain from drk, J. Mol. Biol. 276 (1998) 939–954.
[19] D. Yang, Y.K. Mok, D.R. Muhandiram, J.D. Forman-Kay, L.E. Kay, ^{1}H-^{13}C dipole-dipole cross-correlated spin relaxation as a probe of dynamics in unfolded proteins: application to the DrkN SH_3 domain, J. Am. Chem. Soc. 121 (1999) 3555–3556.
[20] L. Banci, I. Bertini, I.C. Felli, P. Hajieva, M.S. Viezzoli, Side chain mobility as monitored by CH–CH cross correlation: the example of cytochrome *b*5, J. Biomol. NMR 20 (2001) 1–10.
[21] L. Ghalebani, P. Bernatowicz, S. Nikkhou-Aski, J. Kowalewski, Cross-correlated and conventional dipolar carbon-13 relaxation in methylene groups in small, symmetric molecules, Concepts Magn. Reson. A 30 (2007) 100–115.
[22] K.A. Connors, The stability of cyclodextrin complexes in solution, Chem. Rev. 97 (1997) 1325–1357.
[23] J. Kowalewski, G. Widmalm, Multiple-field carbon-13 NMR relaxation study of cyclodextrins, J. Phys. Chem. 98 (1994) 28–34.
[24] D.C. McCain, J.L. Markley, Internal motions of the three hydroxymethyl groups in aqueous sucrose, J. Magn. Reson. 73 (1987) 244–251.
[25] K.E. Köver, G. Batta, J. Kowalewski, L. Ghalebani, D. Kruk, Internal dynamics of hydroxymethyl rotation from CH_2 cross-correlated dipolar relaxation in methyl-β-D-glucopyranoside, J. Magn. Reson. 167 (2004) 273–281.
[26] D.M. Korzhnev, M. Billeter, A.S. Arseniev, V.Y. Orekhov, NMR studies of Brownian tumbling and internal motions in proteins, Prog. Nucl. Magn. Reson. Spectrosc. 38 (2001) 197–266.
[27] M.W.F. Fischer, A. Majumdar, E.R.P. Zuiderweg, Protein NMR relaxation: theory, applications and outlook, Prog. Nucl. Magn. Reson. Spectrosc. 33 (1998) 207–272.
[28] P. Luginbühl, K. Wüthrich, semi-classical nuclear magnetic relaxation theory revisited for use with biological macromolecules, Prog. Nucl. Magn. Reson. Spectrosc. 40 (2002) 199–247.
[29] J. Kowalewski, L. Mäler, Nuclear Spin Relaxation in Liquid: Theory, Experiments and Application, Taylor and Francis, New York, 2006.
[30] H. Wennerström, G. Lindblom, B. Lindman, Theoretical aspects on the NMR of quadrupolar ionic nuclei in micellar solutions and ampliphic liquid crystals, Chem. Scr. 6 (1974) 97–103.
[31] H. Wennerström, B. Lindman, O. Söderman, T. Drakenberg, J.B. Rosenholm, ^{13}C magnetic relaxation in micellar solutions. Influence of aggregate motion on T_1, J. Am. Chem. Soc. 79 (1975) 2283–2292.
[32] G. Lipari, A. Szabo, Model-free approach to the interpretation of nuclear magnetic resonance relaxation in macromolecules. 1. Theory and range of validity, J. Am. Chem. Soc. 104 (1982) 4546–4559.
[33] G. Lipari, A. Szabo, Model-free approach to the interpretation of nuclear magnetic resonance relaxation in macromolecules. 2. Analysis of experimental results, J. Am. Chem. Soc. 104 (1982) 4559–4570.
[34] R.L. Vold, R.R. Vold, Nuclear magnetic relaxation in coupled spin systems, Prog. Nucl. Magn. Reson. Spectrosc. 12 (1978) 79–133.
[35] T.E. Bull, Relaxation in the rotating frame in liquids, Prog. Nucl. Magn. Reson. Spectrosc. 24 (1992) 377–410.
[36] V.A. Daragan, K.H. Mayo, Motional model analyses of protein and peptide dynamics using ^{13}C and ^{15}N NMR relaxation, Prog. Nucl. Magn. Reson. Spectrosc. 31 (1997) 63–105.
[37] J. Kowalewski, M. Effemey, J. Jokisaari, Dipole-dipole coupling constant for a directly bonded CH pair-a carbon-13 relaxation study, J. Magn. Reson. 157 (2002) 171–177.
[38] L. Mäler, J. Lang, G. Widmalm, J. Kowalewski, Multiple-field carbon-13 NMR relaxation investigation on melezitose, Magn. Reson. Chem. 33 (1995) 541–548.
[39] L. Mäler, G. Widmalm, J. Kowalewski, Motional properties of a pentasaccharide containing a 2, 6-branched mannose residue as studied by ^{13}C nuclear spin relaxation, J. Biomol. NMR 7 (1996) 1–7.
[40] D. Canet, S. Bouguet-Bonnet, P. Mutzenhardt, On the calculation of cross-correlation spectral density functions within the model-free approach, Concepts Magn. Reson. A 19 (2003) 65–70.
[41] M.R. Wormald, A.J. Petrescu, Y.-L. Pao, A. Glithero, T. Elliott, R.A. Dwek, Conformational studies of oligosaccharides and glycopeptides: complementarity of NMR, X-ray crystallography, and molecular modelling, Chem. Rev. 102 (2002) 371–386.
[42] C.S. Pereira, D. Kony, R. Baron, M. Müller, W.F. van Gunsteren, P.H. Hünenberger, Conformational and dynamical properties of disaccharides in water: a molecular dynamics study, Biophys. J. 90 (2006) 4337–4344.
[43] C. Ammann, P. Meier, A.E. Merbach, A simple multinuclear NMR thermometer, J. Magn. Reson. 46 (1982) 319–321.
[44] J.S. Blicharski, Nuclear magnetic relaxation in rotating frame, Acta Phys. Pol. A 41 (1972) 223–236.
[45] A.J. Vega, Relaxation in spin-echo and spin-lock experiments, J. Magn. Reson. 65 (1985) 252–267.
[46] J. Kowalewski, A. Ericsson, R. Vestin, Determination of NOE factors using the dynamic Overhauser enhancement technique combined with a nonlinear least-squares-fitting procedure, J. Magn. Reson. 31 (1978) 165–169.
[47] V.A. Daragan, T.N. Khazanovich, A.U. Stepanyants, Cross-correlation effects in multiplet spectra of carbon-13, Chem. Phys. Lett. 26 (1974) 89–92.
[48] L.G. Werbelow, D.M. Grant, Carbon-13 relaxation in multispin systems of the type AX_n, J. Chem. Phys. 63 (1975) 544–556.
[49] C.L. Mayne, D.M. Grant, D.W. Alderman, Structure and dynamics of methylene iodide in solution from nuclear spin-lattice relaxation studies, J. Chem. Phys. 65 (1976) 1684–1695.
[50] R. Behrends, M.K. Cowman, F. Eggers, E.M. Eyring, U. Kaatze, J. Majewski, S. Petrucci, K.H. Richmann, M. Riech, Ultrasonic relaxation and fast chemical kinetics of some carbohydrate aqueous solutions, J. Am. Chem. Soc. 119 (1997) 2182–2186.
[51] J. Stenger, M. Cowman, F. Eggers, E.M. Eyring, U. Kaatze, S. Petrucci, Molecular dynamics and kinetics of monosaccharides in solution, a broadband ultrasonic relaxation study, J. Phys. Chem. B 104 (2000) 4782–4790.
[52] G. Batta, K.E. Köver, J. Gervay, M. Hornyak, G.M. Roberts, Temperature dependence of molecular conformation, dynamics, and chemical shift anisotropy of α, α-trehalose in D2O by NMR relaxation, J. Am. Chem. Soc. 119 (1997) 1336–1345.
[53] K.E. Köver, G. Batta, Separating structure and dynamics in CSA/DD cross-correlated relaxation: a case study on trehalose and ubiquitin, J. Magn. Reson. 150 (2001) 137–146.
[54] Y. Chen, S. Luo, S. Hung, S.I. Chan, D.M. Tzou, ^{13}C solid-state NMR chemical shift anisotropy analysis of the anomeric carbon in carbohydrates, Carbohydr. Res. 340 (2005) 723–729.